REGULAR ARTICLE

blood advances

Elucidating parasite and host-cell factors enabling *Babesia* infection in sickle red cells under hypoxic/hyperoxic conditions

Divya Beri,[1] Manpreet Singh,[1] Marilis Rodriguez,[1] Mihaela Barbu-Stevanovic,[2] Giselle Rasquinha,[3] Avital Mendelson,[4] Xiuli An,[5] Deepa Manwani,[6] Karina Yazdanbakhsh,[7] and Cheryl A. Lobo[1]

[1]Department of Blood-Borne Parasites, Lindsley F. Kimball Research Institute, New York Blood Center, New York, NY; [2]Flow Cytometry and Imaging, Core Facility, Lindsley F. Kimball Research Institute, New York Blood Center, New York, NY; [3]Department of Biology, Georgetown University, Washington, DC; [4]Laboratory of Stem Cell Biology & Engineering Research, Lindsley F. Kimball Research Institute, New York Blood Center, New York, NY; [5]Department of Membrane Biology, Lindsley F. Kimball Research Institute, New York Blood Center, New York, NY; [6]Division of Hematology, Department of Medicine, Montefiore Health Center, Albert Einstein College of Medicine, Bronx, NY; and [7]Department of Complement Biology, Lindsley F. Kimball Research Institute, New York Blood Center, New York, NY

Key Points

- A novel image flow cytometric machine learning tool was developed that robustly identified sickled cells and their constituent hemoglobin.
- Multiple mechanisms of resistance are offered by sickle/sickle trait red blood cells against *Babesia*, especially in low-oxygen environments.

Sickle red blood cells (RBCs) represent a naturally existing host-cell resistance mechanism to hemoparasite infections. We investigate the basis of this resistance using *Babesia divergens* grown in sickle (SS) and sickle trait (AS) cells. We found that oxygenation and its corresponding effect on RBC sickling, frequency of fetal hemoglobin positive (HbF^+) cells, cellular redox environment, and parasite proliferation dynamics, all played a role in supporting or inhibiting *Babesia* proliferation. To identify cellular determinants that supported infection, an image flow cytometric tool was developed that could identify sickled cells and constituent Hb. We showed that hypoxic conditions impaired parasite growth in both SS and AS cells. Furthermore, cell sickling was alleviated by oxygenation (hyperoxic conditions), which decreased inhibition of parasite proliferation in SS cells. Interestingly, our tool identified HbF^+-SS as host-cells of choice under both hypoxic and hyperoxic conditions, which was confirmed using cord RBCs containing high amounts of HbF^+ cells. Uninfected SS cells showed a higher reactive oxygen species–containing environment, than AA or AS cells, which was further perturbed on infection. In hostile SS cells we found that *Babesia* alters its subpopulation structure, with 1N dominance under hypoxic conditions yielding to equivalent ratios of all parasite forms at hyperoxic conditions, favorable for growth. Multiple factors, including oxygenation and its impact on cell shape, HbF positivity, redox status, and parasite pleiotropy allow *Babesia* propagation in sickle RBCs. Our studies provide a cellular and molecular basis of natural resistance to *Babesia*, which will aid in defining novel therapies against human babesiosis.

Introduction

The role of infections in the evolution of their hosts was proposed in 1942 by Haldane.[1,2] This was supported by a wealth of epidemiological data that showed that some human populations have a high incidence of certain genetically inherited diseases, which although harmful, persist in the gene pool. The

Submitted 20 May 2022; accepted 2 August 2022; prepublished online on *Blood Advances* First Edition 17 August 2022. https://doi.org/10.1182/bloodadvances.2022008159.

Data are available on request from the corresponding author, Cheryl A. Lobo (CLobo@Nybc.org).

The full-text version of this article contains a data supplement.

hypothesis proposed by Haldane[1,2] was partly based on his observation that hemoglobinopathies such as sickle cell disease (SCD) have an almost complete geographical overlap with erythrocytic infections such as malaria.[3,4] Thus, parasitic infections could serve as selective forces to shape the genetic structure of human populations. Furthermore, analysis of such mutant red blood cells (RBCs) in comparison with wild-type RBCs can identify host and parasite specific factors crucial for parasite survival and proliferation. For blood-borne parasites, the environment within the host RBC together with its membrane proteins and hemoglobin (Hb), the primary O_2 carrier, are important determinants of parasite success.[5] Pathogenesis of the 2 major human intraerythrocytic parasites, *Plasmodium* and *Babesia*, is intrinsically tied to parasite replication within the RBC followed by the lytic destruction of these cells, leading to anemia and organ damage.[6-10]

The role of RBC polymorphisms, especially sickle cell disorders, in inhibiting malarial infection has been explored for decades, but there is still no consensus on mechanisms of resistance at play in these cells.[11-13] Of the 4 *Babesia* species that can infect humans, *B microti, B divergens, B duncani*, *and B venatorum*, only *B divergens* and *B duncani* can be propagated continuously *in vitro* culture in human RBCs.[14-16] We have focused on *B divergens* to dissect the relationship between this parasitic infection and SCD[5,17] and to understand the mechanisms and pathology that compromise parasite growth in sickle (SS) cells. The single point genetic mutation in the beta chain of globin (Glu6Val) causes the production of abnormal Hb (HbS) in sickle RBCs. According to the Centers for Disease Control and Prevention, it is estimated that 100 000 Americans are affected with SCD, with a disproportionately high incidence in African American births.[18,19] It has been shown that HbS polymerizes under hypoxic and acidotic conditions, which in turn deforms the RBC and lends the cell its characteristic sickle shape.[20] Babesiosis can result in severe hemolytic anemia in patients with SCD, requiring prolonged treatment.[21] Life-threatening complications include acute respiratory failure, disseminated intravascular coagulation, congestive heart failure, coma, and adrenal failure.[22] Despite treatment, individuals with SCD are also likely to develop persistent relapsing disease.[23] Although, asplenia may contribute to the severity of their symptoms,[24,25] other aspects of the disease severity remain poorly investigated.

Previously, we have shown that under standard parasite culture conditions using 5% O_2, the propagation of *Babesia* was severely compromised in SS cells compared with growth in wild-type (AA) or sickle trait (AS) cells.[17] Although, sequestration has not been documented for *B divergens*, the infected RBCs of a related parasite *B bovis* have been shown to sequester in the host microvasculature, in vital organs such as brain, bone marrow, and spleen, where O_2 levels fall dramatically.[26-28] Further, hypoxia is known to significantly enhance RBC adherence.[29,30] Thus, because the concentration of O_2 varies throughout the body with higher arterial concentrations and lower concentrations in most organs of the body[30,31] and is also known to contribute to the change in shape of sickle cells,[32] we explore the effect of differential O_2 on the growth and population dynamics of *Babesia* in SCD and sickle cell trait RBCs compared with wild-type normal trait (AA) cells.

Using human sickle, sickle trait (AS), or control RBCs as hosts for *Babesia* infection, we show that multiple factors including oxygenation, its differential effect on the shape of the wild-type and mutated RBCs, and the proportion of fetal Hb positive (HbF^+) cells affect both the choice of host cell that the parasite grows in as well as the proliferation dynamics of *Babesia* populations in these Hb variant cells. Specifically, cells from individuals with SCD exhibit great diversity with respect to shape, sickling, and both percentage of HbF^+ cells and amounts of HbF per cell, allowing us to examine the association of these SCD cell-specific features with parasite hosting. To accurately assess the relationship among oxygenation, HbF, and sickling of cells in relation to parasite infection, a robust image flow cytometry (IFC)–based, observer-independent machine learning (ML) algorithm was developed to identify sickle-shaped cells using Luminex's ImageStream Data Exploration and Analysis Software (IDEAS). This allowed us to identify specific cells in the SCD cultures that supported *Babesia* proliferation. Furthermore, we explored the link between differences in the cellular redox environments of these different sickle genotypes and their impact on parasite development. The results were used to explore potential cellular mechanisms in both the parasite cell and host RBC that may play a role in dictating the success in establishing these infections.

Materials and methods

Detailed experimental procedures have been included in supplemental Methods.

B divergens in vitro culture

B divergens (Bd Rouen 87 strain) was maintained in human RBCs at 5% hematocrit in complete RPMI, as previously described.[33,34]

Assessment of invasion, development, and egress in various RBCs

Invasion and development of parasites in RBCs were measured using flow cytometry and light microscopy of Giemsa-stained slides smeared with RBCs from culture every 24 hours.

IFC and ML module in IDEAS

RBCs were incubated overnight at 5% hematocrit under standard or specific O_2 conditions, and 50 μL of culture was immediately added to a tube containing previously deoxygenated 0.05% glutaraldehyde in phosphate-buffered saline (PBS) and kept at room temperature for 10 minutes in a glovebox at the respective O_2 condition. This was followed by washes in 1% bovine serum albumin/PBS and permeabilization with 0.1% Triton X 100 for 3 minutes at room temperature. After 3 washes in 0.1% bovine serum albumin/PBS, the respective antibody/dye was added. After staining, images were acquired using a 12-channel Amnis brand ImageStreamX Mark II (Luminex, Austin, TX) IFC. Samples were acquired at 60× magnification at low speed, and the excitation lasers 405 (violet), 488 (green), and 642 nm (red) were set at the required power. Brightfield images were acquired in Channels 1 and 9, whereas side scatter was acquired in channel 6. Image analysis was performed by using image-based algorithms in IDEAS 6.3.

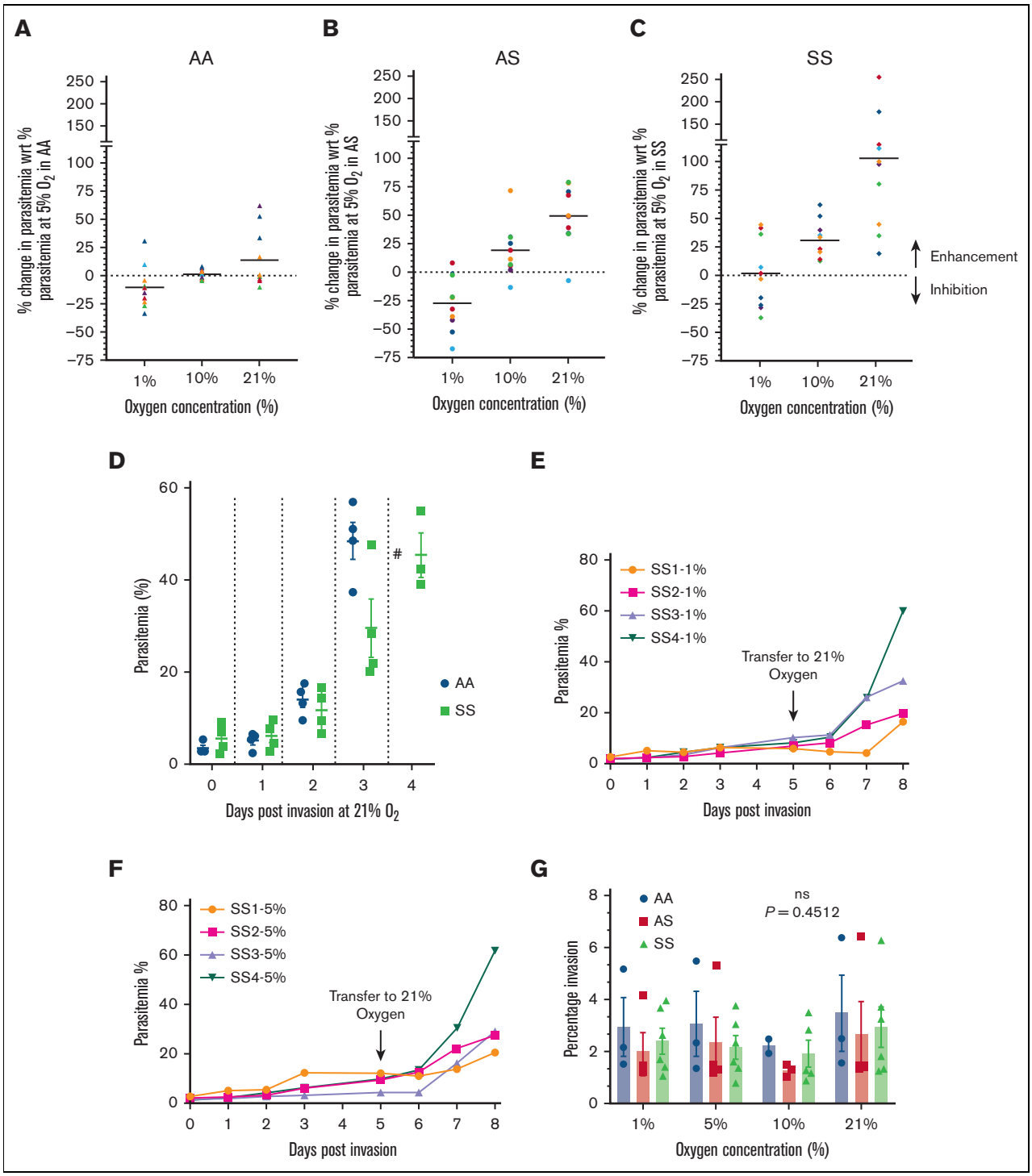

Figure 1. Examining growth of *B divergens* in different RBC genotypes at different O_2 concentrations. *B divergens* was grown synchronously *in vitro* at 1%, 5%, 10%, and 21% O_2, with constant 5% CO_2 and remaining N_2. Three genotypes were examined: (A) AA wild type, (B) AS heterozygous for SCD and (C) sickle (SS) homozygous for SCD. Parasitemia at day 3 after invasion were plotted as the percentage of enhancement or inhibition compared with its own growth at standard 5% O_2 used widely for *in vitro* cultures. As evident in (A), parasites grown at 1% O_2 in AA cells showed similar growth as 5% O_2 (moderate, nonsignificant inhibition of 10.05% ± 5.97%). At 10% and 21% O_2, the growth was enhanced (1.39% ± 1.37%, $P = .1559$ and 13.91% ± 8.41%, $P = .0467$, respectively). For parasites growing in AS RBCs (B), there was a significant inhibition of growth at 1% O_2 (26.48% ± 8.27%). At 5% O_2, AA and AS growth rates were comparable. Similar to AA cells, AS cells exhibited enhanced growth at 10% (25.38% ± 7.23%) and 21% O_2 (47.9% ± 7.96%). (C) For the SS genotype, at 1% O_2, parasites were inhibited almost unchanged as compared with 5% O_2 at which parasites also suffered from impaired growth. However, at higher O_2 levels, parasites grew better, as shown by a 31.34% ± 5.03% and 101.29% ± 21.46% enhancement of growth compared with 5% at 10% and 21%, respectively. (D) The percentage of parasitemia is plotted for AA and SS cells grown at 21% O_2 over days after the invasion. As shown, starting from day 2, AA

Redox assays

Two redox assays were used. CellROX Deep Red (ThermoFisher Scientific C10491) was used at 1:1000 to stain cells for 45 minutes at 37°C in 96-well plates, and live cells were immediately analyzed in a BD flow cytometer equipped with a 640-nm laser or a Zeiss LSM 880 with Airyscan confocal microscope images taken using a 63× objective lens.

For the DCFDA (2′, 7′-dichlorofluorescin diacetate; Abcam ab113851) assay, cells were incubated in a 1:1000 DCFDA solution in a colorless incomplete medium for 30 minutes of incubation at 37°C in the dark and analyzed in a BD flow cytometer.

Results

Level of oxygenation impacts parasite growth in different sickle Hb variant cells

We hypothesized that O_2 levels may influence the shape of the sickle cells with concomitant effects on the growth of *B divergens*. Synchronized parasite cultures were grown in different O_2 environments (1%, 5%, 10%, and 21% O_2), 5% CO_2, and the remaining in N_2, after the merozoite invasion. Our results (Figure 1A-C; supplemental Figure 1) indicate that the degree of oxygenation plays a role in the degree of parasite proliferation in all Hb variants. Day 3 was chosen for analysis, as it represents peak parasitemia in AA cells, whereas day 4 parasitemia in AA cultures generally go more than the support level of the culture system (crashed). All graphs in Figure 1A-C compare the inhibition (negative value on the y-axis) or enhancement (positive value on the y-axis) of parasite growth in each specific culture as compared with its standard 5% O_2 growth as measured on day 3 after the invasion. Supplemental Figure 1 shows the absolute parasitemia obtained in each sample of host AA, AS, and SS cells (n = 10 for each) on day 3 after the invasion at all different O_2 concentrations for all the sample points tested. Both the parasitemia within different O_2 conditions in the 3 host-cell genotypes as well as between genotypes differed significantly ($P = .003$).

AA cells exhibited higher parasitemia at all O_2 concentrations, compared with AS or SS cells (Figure 1A; supplemental Figure 1). As shown in supplemental Figure 1, the absolute parasitemia in AA cells at 1%, 5%, 10%, and 21% O_2 were 33.951% ± 3.214%, 37.749% ± 2.815%, 38.201% ± 2.7%, and 41.57% ± 2.69%, respectively, exhibiting increasing parasitemia with increasing O_2. Percentage inhibition or enhancement at 1%, 10%, and 21% O_2 as compared with each sample's standard 5% culture conditions, as shown in Figure 1A, reveals a nonsignificant inhibition at 1% and 10%. At 21%, there was a significant increase in parasitemia of ~14% ($P = .0467$).

The absolute parasitemia in AS cells in 1%, 5%, 10%, and 21% O_2 were 24.04% ± 2.61%, 33.36% ± 1.507, 41.44% ± 2.34%, and 48.607% ± 2.098%, respectively (supplemental Figure 1). Previously, we had not been able to differentiate between AS and AA cells as optimum host cells for *B divergens* at standard 5% O_2.[17] However, lowering the O_2 concentration to 1% (hypoxia) permitted genotype-based discrimination. AS cells at 1% O_2 were not able to support parasite growth as efficiently as AA cells (see Figure 1B; supplemental Figure 1 for AS cells). Inhibition of parasite growth of 26.48% ± 8.277% was observed in AS cells relative to 5% O_2. However, increasing the O_2 levels removed this inhibition, and at 10% O_2, we found a 25.38% ± 7.23% enhancement of parasitemia ($P = .0002$, n = 10), which further increased by 47.9% ± 7.96% when O_2 levels were increased to 21% ($P = .0001$, n = 10).

The effect of oxygenation on parasite growth in the SS genotype is shown in supplemental Figure 1 and Figure 1C. The absolute parasitemia obtained were 10.716% ± 1.744%, 11.627% ± 2.533%, 15.683% ± 3.844%, and 23.769% ± 5.910% at 1%, 5%, 10%, and 21% O_2, respectively. Although 5% O_2 confirmed the previously reported relative resistance of SS cells to infection by *B divergens*, we showed that lowering the O_2 concentration to 1% did not yield much difference. Importantly, increasing the O_2 saturation helped alleviate the inhibition, with growth at 10% O_2 enhancing growth of parasites in SS cells by 30.440% ± 5.275% than that at 5% O_2. Remarkably, at 21% O_2, we see an almost complete rescue of the inhibition, with an enhancement of parasite growth of 101.29% ± 21.46%, allowing parasitemia to approach that of wild-type AA cells, albeit at a slower rate. To investigate whether parasitemia in SS cells can approach those seen at peak levels in AA cells, we followed infection in AA and SS cells (n = 4). On day 3, after the invasion (Figure 1D), in a 21% O_2 environment, AA cells reached a peak parasitemia of 48.423% ± 4.105%, whereas in SS cells, parasitemia was lower, 29.458% ± 6.337% (n = 4). However, parasitemia reached a peak value of 45.367% ± 4.866% on day 4 in SS cells at 21% O_2, whereas parasites in AA "crashed" on day 4 due to insufficient numbers of host cells left in culture (shown by "#"). Thus, SS cells can support high parasitemia similar to AA cells at 21% O_2, but a longer time was required to achieve this peak parasitemia.

To analyze whether the merozoites produced in hypoxic SS cells could initiate productive asexual cycles, we assessed the rescue by transferring parasites grown at lower O_2 conditions (1% and 5%) in SS cells to 21% O_2 (Figure 1E-F). Parasites were transferred from 1% and 5% O_2 cultures of infected SS cells on day 5 of growth in hypoxic conditions (average parasitemia before transfer was 7.87% ± 0.948% and 9.053% ± 1.6%, respectively). After the transfer, the parasitemia did not change significantly on day 6 (8.58% ± 1.477% and 10.313% ± 2.055% for 1% and 5% O_2, respectively). But, on days 7 and 8, parasites showed near-normal growth patterns and for 1% and 5% O_2, reached parasitemia of 32.27% ± 9.843 and 34.848 ± 9.180%, respectively. Thus, parasites that had shown stagnated growth in hypoxic culture

Figure 1 (continued) cells support better growth of parasite, and this difference is evident at day 3, when parasites in AA cells reach their peak, *in vitro* parasitemia of 48.423% ± 4.105%, whereas parasites in the SS cells are at 29.458% ± 6.337% parasitemia. On day 4, the AA culture crashed (as shown by #), whereas the SS culture reached its peak of 45.367% ± 4.866%. (E and F) Transfer experiments: parasites were grown at 1% O_2 (E) and 5% O_2 (F) and on day 5 after the invasion at parasitemia of 7.87% ± 0.948% and 9.053% ± 1.6%, respectively, were transferred to 21% O_2. After transfer, parasites previously grown at 1% and 5% reached parasitemia of 32.27% ± 9.843% and 34.848% ± 9.180%, respectively. Thus, after stagnation of growth at low- O_2 conditions, transfer to a higher O_2 condition can rescue the growth of the parasites to near-normal levels in SS host RBCs. (G) We examined whether parasite invasion was affected by different O_2 levels across the 3 genotypes. No significant differences were found ($P = .4512$), thus suggesting that the invasion of *B divergens* remains similar across genotypes and at different O_2 culture conditions.

conditions could be rescued to near-normal growth levels when O_2 levels were increased, suggesting that the viability of parasites in SS cells at low O_2 are similar to those produced both in high-O_2 environments as well as those produced from other genotypes, and on return of favorable hyperoxic conditions, they grow to near-normal levels.

Parasite invasion is mediated by interactions between the merozoites and the surface proteins of the RBCs.[35] As the shape of the sickle RBC is affected by their O_2 load, we next assessed whether incubating the SS cells in a low-O_2 (1%) environment would affect the ability of merozoites to invade these RBCs. Cells were incubated overnight in different O_2 conditions to ensure saturation of cells with the gas at specific concentrations after merozoite invasion at these O_2 levels. As seen in Figure 1G, similar invasion efficiencies were obtained for SS cells across all O_2 levels. Our results, therefore, indicated that the invasion efficiency into hypoxic cells was not a factor in the low parasitemia obtained subsequently in SS cells at low-O_2 levels.

Redox imbalance in host SS cells may contribute to the growth defect of *Babesia* under standard culture conditions

As redox imbalance is a known hallmark of sickle RBCs,[36] we examined its role in the differential growth of *B divergens*. We measured reactive oxygen species (ROS) in AA vs AS vs SS cells using both flow cytometry–based CellROX Deep Red (CRR) reagent and DCFDA. Although CRR is more reactive toward superoxides in the cytoplasm of live cells, DCFDA is oxidized by the hydroxyl species, peroxyl species, and other ROS.

At standard culture conditions (5% O_2), invasion of *B divergens* into RBCs was performed, with media change every 24 hours. Redox assays for day 2 are presented. For CRR, Hoechst (HO) staining was performed to differentiate the source of signal from uninfected or infected cells. As shown in Figure 2A, the mean ± standard error of the mean for uAA and uAS were 0.54% ± 0.15% and 0.33% ± 0.15% ($P = .3370$, nonsignificant), respectively, whereas for uSS the value was 6.30% ± 1.77% ($P = .0018$, n = 11). For infected cells, we normalized the CRR signal to parasitemia because the different genotypes supported differential growth of the parasite (explained in Figure 1). On normalization, we observed that CRR signal in iSS was 2.055 ± 0.56, almost 3 times the signal of iAA and iAS, which had values of 0.63% ± 0.07% and 0.69% ± 0.06% ($P = .028$, n = 15), respectively. Furthermore, in our flow data plots, using CRR^+ cells as our parent gate and assaying the DNA positivity (HO) of the cells, we observed that for AA and AS, the CRR signal originated almost exclusively from cells that harbored *Babesia* indicated by HO positivity (87.5% ± 2.5% and 88.9% ± 2.05%, respectively) as opposed to SS, in which of all CRR^+ cells, only 42.7% ± 4.1% cells were parasite positive. To visually confirm this, confocal microscopy was performed on uninfected and infected cells (Figure 2C). We observed that uAA had no CRR signal as opposed to uSS cells, signal marked by black arrows in Figure 2C. On infection, the CRR signal was localized exclusively to the parasite-infected cells with no signal in bystander cells, whereas in SS, uninfected bystander cells were also stained by CRR (marked by a black arrow), in addition to the ones infected by the parasite (Figure 2C).

Next, we observed that the DCFDA signal in uSS and iSS was also higher than that recorded in uAA and iAA, respectively, as shown by the right shift of the histogram for DCFDA in Figure 2D. Both flow cytometry and microscopy standard culture conditions of 5% O_2 confirmed that SS RBCs present a more oxidizing and higher ROS-containing environment than AA and AS RBCs.

Redox imbalance persists across O_2 levels in SS genotype uninfected and infected RBCs

Having established that SS cells have an imbalance in redox homeostasis under standard culture conditions (5% O_2, Figure 2), we investigated whether the increase in parasitemia at hyperoxic conditions can be attributed to modulation of redox parameters under those conditions to provide a more favorable environment for parasite propagation.

The parasites were grown at 1%, 5%, 10%, and 21% O_2 with uninfected cells maintained under identical conditions. Redox analysis of samples on day 2 is presented. As shown in Figure 3A, across all O_2 levels, CRR signals in uAA and uAS were low with uAA CRR positivity of 0.49% ± 0.216%, 0.544% ± 0.153%, 1.03% ± 0.589%, and 0.597% ± 0.339% at 1%, 5%, 10%, and 21% O_2, respectively. Similarly, in uAS, CRR^+ cell percentages were 0.335% ± 0.168%, 0.330% ± 0.152%, 0.520% ± 0.268%, and 0.563% ± 0.355% at 1%, 5%, 10%, and 21% O_2, respectively. The examination of uSS cells revealed a fivefold increase in CRR positivity, with values of 5.21% ± 1.41%, 4.743% ± 0.940%, 6.514% ± 2.189%, and 3.813% ± 0.931% of all single cells at 1%, 5%, 10%, and 21% O_2, respectively. Of note, the difference in CRR positivity of uSS within different O_2 levels was not statistically significant with a P value of .6227, indicating that the increase in O_2 levels in cultures did not contribute to the increase in CRR positivity.

Because the different sickle genotypes harbored different percentages of parasites, we normalized CRR levels to parasitemia and calculated the percentage of CRR-positive cells (CRR^+) per the percentage of parasite-harboring cells. As shown in Figure 3B, across all O_2 levels, CRR^+ iAA and iAS cells normalized to parasitemia were low (<1% cells) and comparable and not statistically significant across all O_2 levels. However, for iSS cells, CRR positivity was found to be almost 3 times higher at all O_2 levels. As evident from the graph, the number of CRR^+ cells decreased slightly at 21% O_2, but the differences within iSS at different O_2 levels were not statistically significant ($P = .5829$). Overall, infection in SS cells resulted in a significantly higher number of CRR^+ cells than AA and/or AS cells ($P < .0001$).

Confirmation of these redox differences was obtained visually by analysis of the confocal images for these cells stained with CRR (red) and Vybrant DyeCycle (FITC channel: green). For iAA cells (Figure 3C), only infected cells (green) were positive for CRR (red) across all O_2 levels with similar intensity. By contrast, in iSS cells (Figure 3D), we observed several uninfected cells (no DNA/FITC signal) that fluoresced bright red, indicative of ROS buildup in these cells, (black arrowheads). Therefore, in iSS, bystander cells that are potential hosts for egressing parasites do not provide a hospitable environment and may account for reduced parasitemia in SS cells at low O_2 levels and a lag in parasite growth at hyperoxic conditions (Figure 1D). Similar to iAA, all parasitized SS cells were found to be CRR^+.

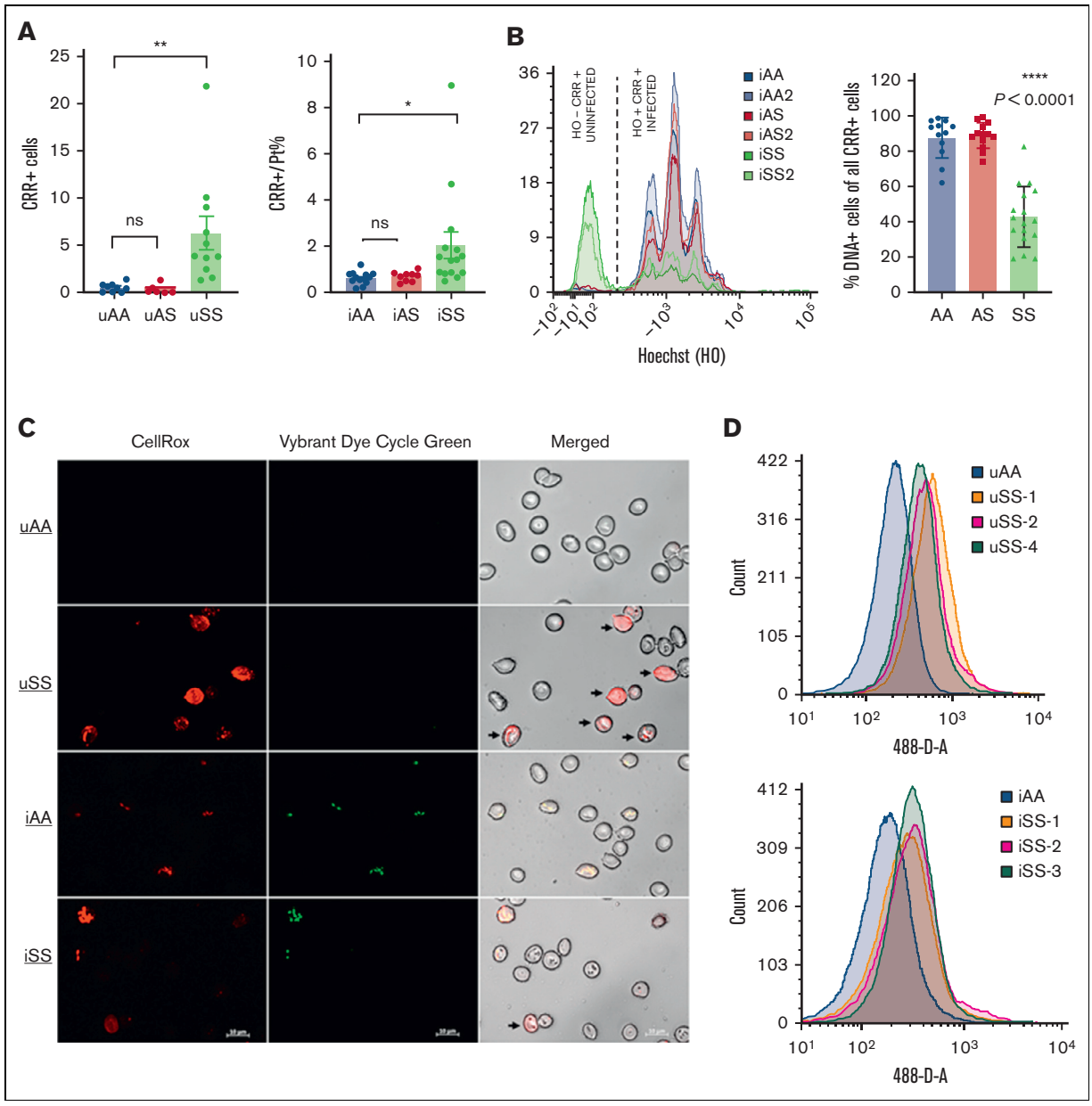

Figure 2. Redox imbalance in host SS cells may provide a less hospitable environment for *Babesia*: *B divergens* was cultured under standard culture conditions in AA, AS, and SS cells. Redox assays were performed on day 2 after the invasion. (A) Using a cell-permeant and cytoplasm-specific redox dye CRR, we quantified the percentage of cells with ROS. Left panel: uAA and uAS had negligible levels of ROS, whereas that of uSS was almost sixfold higher ($P = .0018$, n = 11). Right panel: different genotypes exhibit differential parasitemia (Pt%); thus, for infected cells, we normalized CRR signal to Pt%; iSS signal was threefold higher than iAA and iAS ($P = .028$, n = 15). (B) Cells were stained with HO (DNA dye which is equivalent to Pt% in a nucleus-free RBC) and CRR. Cells positive for CRR were used as parent gate and checked for HO positivity. For iAA, iAS, and iSS, most CRR^+ cells were HO^+, whereas only in uSS samples, they showed CRR signal. This was quantified in the graph where y-axis represents the percentage of HO^+ cells in the CRR^+ population in each of the genotypes. As shown, in AA and AS cells, there was almost complete coincidence of oxidative stress in infected (HO^+) cells, whereas in SS cells, only 42.7% ± 4.1% CRR^+ cells harbored parasites ($P < .0001$). (C) Cells were stained with CRR (red) and Vybrant DyeCycle (fluorescein isothiocyanate [FITC]) DNA dye, and confocal microscopy was performed using 63× magnification using Zeiss LSM 880 with Airyscan. As shown in the image, uAA had no CRR signal, but several uSS showed positivity for CRR (marked with black arrows). In iAA, the ROS signal coincided completely with cells harboring the parasite, whereas in iSS, uninfected bystander cells also showed fluorescence (marked in black arrows). Thus, imaging of these cells strengthens our findings and provides a visual picture of our flow data. (D) Cells were stained with DCFDA, a redox dye which detects hydroxyl species, peroxyl species, and other ROS species within cells, detected in the 488-D channel in BD Fortessa flow cytometer. As shown in histogram overlays, both uSS and iSS (orange, pink, and green shading) were right shifted compared with uAA and iAA (in blue), respectively. Scale bars = 10 μm.

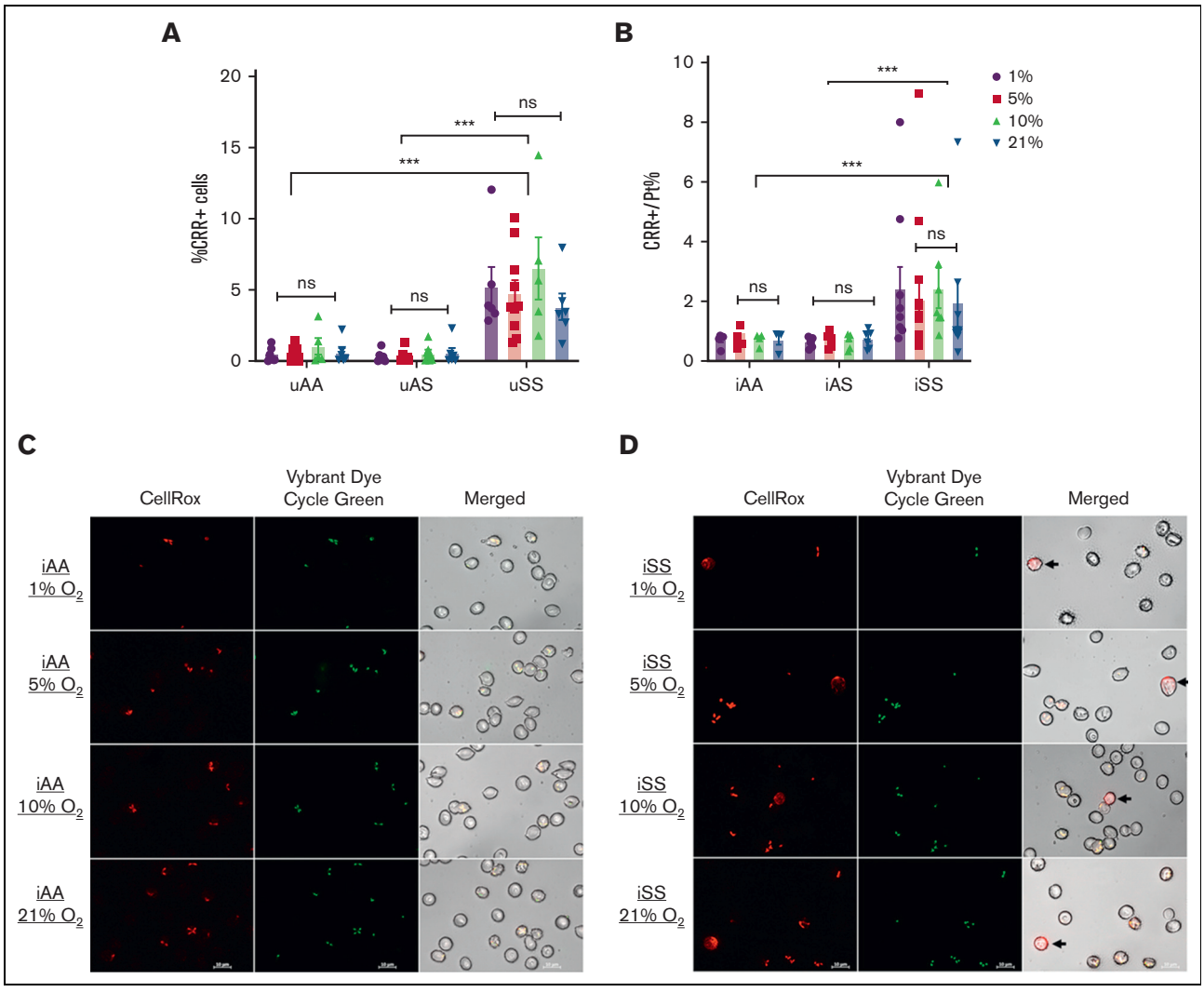

Figure 3. High oxidative stress in SS cells persists across culture conditions with different O_2 concentrations. (A) uAA, uAS, and uSS cells were examined for CRR. The percentage of CRR^+ cells (y-axis) was low in uAA and uAS cells and similar across all O_2 levels ($P = .5021$). As expected, uSS cells had a higher percentage positivity for CRR, almost fourfold higher than uAA ($P < .0001$). However, between O_2 conditions, the percentage of CRR^+ cells in uSS did not change significantly ($P = .6227$). (B) A similar trend was seen in CRR^+ cells normalized to parasitemia in iAA, iAS, and iSS cells. Although iAA and iAS cells had low positivity for CRR, iSS cells had 2.5-fold more CRR^+ cells, as compared with iAA and iAS ($P < .0001$). This also indicates that most of the CRR positivity in iAA and iAS originates from parasite-harboring cells, because when normalized to parasitemia, they showed very few cells as CRR^+. (C) Confocal images of iAA at 1%, 5%, 10%, and 21% O_2 levels and stained with CRR (red) and Vybrant DyeCycle (FITC). The images indicate complete colocalization between parasite (seen clearly in their classical 1N, 2N, or 4N forms) and CRR signal. Thus, ROS in iAA cells is mostly restricted to infected cells, and surrounding bystander cells have nondetectable levels of oxidative species. (D) Confocal images of iSS at 1%, 5%, 10%, and 21% O_2 levels and stained with CRR (red) and Vybrant DyeCycle (FITC). The images across different O_2 levels indicate presence of CRR signal in uninfected cells (shown in black arrows) and in addition, colocalization between parasite and CRR signal. Scale bar = 10 μm.

Thus, we conclude that although redox imbalance is a hallmark of both uninfected and *Babesia*-infected SS cells across all O_2 levels, differences in ROS across O_2 levels were not significant and could not explain the considerable differences in parasitemia in SS cells recorded in 5% and 21% O_2 culture environments (Figure 1C).

Application of ML and IFC to detect shape differences under hypoxic and hyperoxic conditions in SS RBCs

The percentage of RBCs undergoing sickling *in vitro* varies largely across different SCD genotypes and their environmental niche.[37,38] Classically, light microscopy with manual counts has been used to detect sickling. Researchers have used image cytometry to detect sickling in hypoxic conditions for SS cells using cell-based parameters.[39] The advantage of using IFC is that it can detect multiple fluorescent markers along with cellular morphology, allowing us to study the specific characteristics of SS cells. We combined IFC with ML to classify SS cells as "sideways," "sickle," or "round." Cells classified as "sideways" were excluded from further analysis. Thus, the ML algorithm can be used without user bias in multiple samples. The methodology is explained under "Materials and methods" and supplementary information

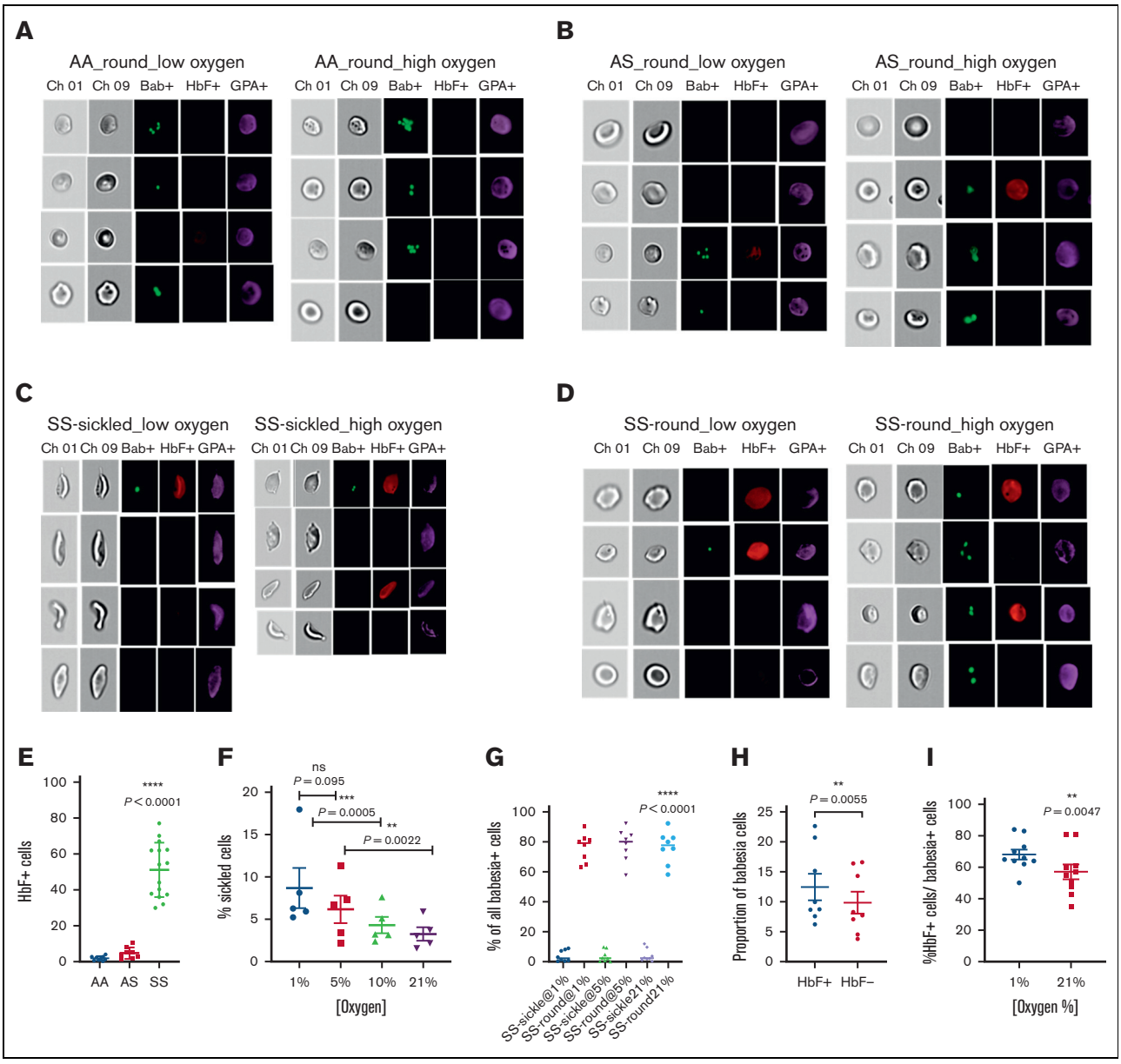

Figure 4. Shape of RBCs affects parasite proliferation in SS cells. (A) AA RBCs infected with *B divergens* were imaged at day 3 of infection. More than 99% of the cells were classified as "round" by the ML algorithm as shown in the representative images. Cells were stained with anti-GPA (violet), Vybrant Green (nucleus of *Babesia*), and anti–HbF-APC. All cells expressed GPA, and *Babesia* was seen as green dots in the cells with 1N, 2N, and 4N nuclei. (B) AS cells were similarly stained and analyzed by image cytometry. More than 98% of the cells were classified as "round" by the ML algorithm, and *Babesia* was seen as green dots in the cells with 1N, 2N, and 4N nuclei. (C-D) SS cells were stained similarly and imaged at low O_2 (C) and high O_2 (D) conditions. A fraction of cells appeared as sickled at both concentrations, although the "sickle" population was significantly higher at low O_2 conditions, as shown in the images. Most SS cells that were classified as "sickle" did not harbor the parasite, and for the few which did, the DNA content was usually always found to be 1N. The "round" cells classified in SS RBCs were shown to be the predominant cell harboring the parasite. (E) The percentage of cells expressing HbF was plotted (mean ± standard error of the mean) for AA (1.843 ± 0.4087), AS (4.755 ± 1.123), and SS (51.17 ± 1.123). The difference in HbF^+ cells was statistically significant among the genotypes. (F) The percentage of cells that were classified as "sickle" by the ML algorithm was plotted at different O_2 levels for *Babesia*-infected SS cells (n = 5). The percentage of sickling cells reduced as the cells were incubated at higher O_2 levels, and this change was statistically significant ($P = .0357$). (G) *Babesia*-infected cells were gated and then checked for "sickle" or "round" shape in infected SS samples. As evident from the graph, almost all *Babesia*-infected host SS cells were "round" and not "sickle" with a P value of <.0001. Differences in these were not significant between different O_2 concentrations; therefore, across all different O_2 concentrations tested, *Babesia* invaded "round" cells more often than "sickle" cells. (H) The proportion of *Babesia*$^+$ cells in normalized HbF^+ or normalized HbF^-- cells grown under 1% O_2 was calculated. Thus, if HbF^+ and HbF^- cells are present in similar numbers, parasites prefer HbF^+ cells over HbF^- cells ($P = .0055$, n = 8). (I) Comparison of the percentage of all parasitized cells that are HbF^+ at 1% and 21% O_2. As compared with parasites at 1% O_2, parasites at 21% O_2 seem to have a diminished preference for HbF^+ cells ($P = .0047$, n = 10). Scale bar: Enlarged Brightfield (BF) image shown beside Fig. 4C.; scale = 7 μm.

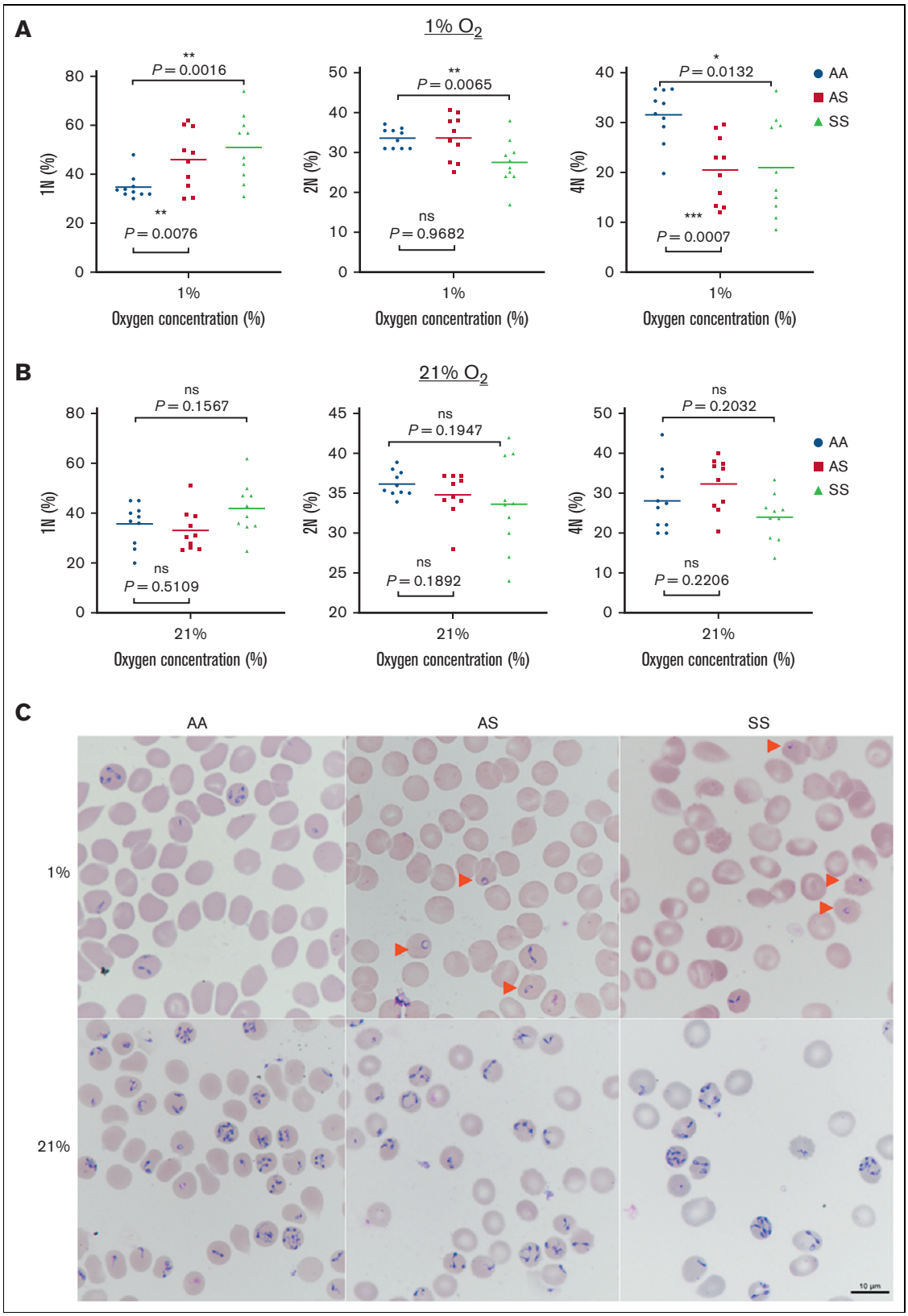

Figure 5. Examination of changes in parasite population structure when grown in different RBC genotypes and under different O_2 conditions. Parasite subpopulations exist as 1N, 2N, or 4N and >4N and in wild-type cells are maintained at ~ 33%:33%:33%. (A) Represents subpopulations at 1% O_2; (B) represents 2N subpopulations at 21% O_2. Within the AA genotype, the population structure of growing parasites is almost equally divided between 1N, 2N, and together 4N and >4N. As evident

(supplemental Figure 2; supplemental Table 1A-C) It provides details of the "classifiers" used by the ML algorithm to distinguish between "sideways," "round," and "sickle" cells.

uAA, uAS, and uSS were incubated at different O_2 conditions for 12 hours after fixation and staining, as described under "Methods." As seen in supplemental Figure 3A-B, AA and AS genotypes showed only the "round" forms. Adult AA and AS cells have low HbF^+ cells. All the cells were glycophorin A-positive (GPA^+), which ensured that there was no contamination of other blood cells. For SS samples, we observed heterogeneity in a fraction of samples such as "sickle" and "round" (supplemental Figure 3C-D).

Under deoxygenated conditions, HbS undergoes a marked decrease in solubility, increased viscosity, and polymer formation, which promotes sickling. Therefore, we quantified percentage of "sickled" cells in SS cells at 1%, 5%, 10%, and 21% O_2 (supplemental Figure 3E), and these were 8.528% ± 1.985%, 4.530% ± 0.694%, 4.228% ± 0.585%, and 3.140% ± 0.83%, respectively, showing an expected decrease in the percentage of sickled cells with increasing O_2 levels.

Next, we measured the percentage of HbF^+ cells in SS samples, as HbF has been inversely correlated with a "sickle" shape.[39] In most individuals with SCD being treated with hydroxyurea, HbF levels increase; however, the magnitude of this increase varies, allowing a range of HbF-expressing cells in the SS pool. Using anti-GPA anti-HbF antibody, we assessed the impact of the presence of HbF on the shape of the cell. As shown in supplemental Figure 3F, of all HbF^+ cells, "sickle" cells contributed a very small percentage across all O_2 environments as marked by SS-sickle@O_2. At 1%, 5%, 10%, and 21% O_2, the fraction of HbF^+ cells, which were classified as "sickled" by our ML algorithm, was 6.495% ± 3.249, 6.498% ± 4.585, 4.418% ± 2.626, and 5.828% ± 3.983, respectively. Therefore, there is a negative correlation between HbF positivity and "sickling."

The shape of host RBCs appears to play an important role in host-cell selection by *B divergens* in SS cells

Next, we exploited the ML algorithm to identify whether there was a subset of cells in the SS cultures that were preferential hosts for *B divergens*. IFC was performed on *B divergens*–infected RBCs from parasite cultures. As seen in Figure 4A, iAA cells at high and low O_2 levels were all classified as "round," and cells lacking HbF^+ cells (red) (1.843% ± 0.41% HbF^+, Figure 5E). All cells were stained with GPA (violet). Analysis of AS RBCs (Figure 5B) revealed that almost all cells were classified as "round" by our ML algorithm. Although a previous paper showed that HbS polymerization increased in *Plasmodium*-infected AS cells,[12] we were not able to detect any shape change in *Babesia*-infected AS cells by using IFC-based ML. HbF^+ cells were detected at 4.755% ± 1.123% (Figure 4E). Therefore, we did not find any significant differences in this analysis of HbF^+ cells and infection between iAA and iAS across all O_2 conditions.

Next, we examined iSS cells. Similar to uSS cells, we observed a heterogenous mixture at low and high O_2 levels of "$sickle^+$" and "$round^+$" cells as shown in Figure 4C-D, respectively. HbF^+ cells were significantly higher in most SS samples examined, with a mean of 51.17% ± 3.926% HbF^+ cells; $P < .0001$ (Figure 4E). As shown in Figure 4F, with increasing O_2 levels, sickling decreased significantly ($P = 0027$ with the percentage of sickled cells at 1%, 5%, 10%, and 21% O_2 recorded as 8.726% ± 2.353%, 6.224% ± 1.613%, 4.338% ± 0.94%, and 3.306% ± 0.7531%, respectively, of the total "no sideways" cells). The difference in the percentage of sickling between 1% and 5% O_2 was not significant ($P = .095$; in line with similar parasitemia obtained at 1% and 5% in SS cells) but between 1% and 10% ($P = .0005$) and 5% and 21% ($P = .0022$) was significant.

Furthermore, as seen in Figure 4G, of all $Babesia^+$ cells, a very low percentage were "sickle" shaped at all O_2 concentrations. At 1%, 5%, and 21% O_2, the percentage of $Babesia^+$ RBCs that were "$sickle^+$" was 3.864% ± 1.291%, 3.823% ± 1.372%, and 4.184% ± 1.514%, respectively, and these differences were not statistically significant. Thus, across all O_2 environments, $Babesia^+$ host RBCs were "round." Therefore, the shape of the SS cells, which is expectedly affected by O_2 levels, may dictate the differences in parasitemia levels recorded in SS cells under different O_2 levels as detailed in Figure 1C.

Next, we calculated the proportion of $Babesia^+$ cells under hypoxic culture conditions, normalized to HbF^+ or HbF^- cells (supplemental Methods). As shown in Figure 4H, parasites have ~1.6-fold preference for HbF^+ cells than HbF^- cells at 1% O_2 ($P = .0055$). The range of values obtained in Figure 5H may reflect the different amounts of HbF per cell, although this is not easy to quantify. This preference of the parasite for HbF^+ cells is after normalization of the respective populations, and therefore, in an SS sample that has higher HbF^+ cells (as shown in Figure 4E), parasitized HbF^+ cells will have an even more dominant profile.

To understand the parasite's preference for HbF^+ or HbF^- cells in any given SS sample (with a constant number of HbF^+ cells) compared with low- and high-O_2 conditions, we examined the percentage of cells that were HbF^+ of all infected cells at low- and high-O_2 conditions. As shown in Figure 4I, the percentage of HbF^+ cells of all $Babesia^+$ cells at 1% O_2 was 68.10% ± 3.188% and reduced to 57.10% ± 4.716% at 21% O_2. Therefore, for a given SS sample with a fixed number of HbF^+ cells, parasites preferentially invade HbF^+ cells at 1% O_2 and 21% O_2, but at 1% O_2, the

Figure 5 (continued) from the graphs, within the AA RBCs, the population structure was similar across both O_2 conditions. (A) When grown in AS cells, parasites had a higher percentage of 1N at 1% O_2 (46.09% ± 3.84%) and significant reduction in 4N populations as compared with AA (20.479% ± 2.12% in AS vs 31.529% ± 1.73% in AA). For SS RBCs, at 1% O_2 (hypoxia), 1N contributes 51.006% ± 4.298% to the population structure, thus explaining the stunted growth at these hypoxic conditions. (B) At 21% O_2, 1N, 2N, and 4N of AS changed to 33.09% ± 2.58%, 34.78% ± 0.89%, and 32.27% ± 2.066%, respectively, which is largely similar to the wild-type AA 33%:33%:33% pattern. In SS host cells, parasite subpopulations exhibit a major recovery compared with 1% O_2 with 1N, 2N, and 4N at 41.82% ± 3.26%, 33.625% ± 1.829%, and 23.977% ± 1.829%, respectively. None of these at 21% O_2 are statistically significant when compared with parasite structures in AA cells. (C) Giemsa-stained images of parasites grown in AA, AS, and SS RBCs at 1% and 21% O_2. As evident in representative images, at lower O_2 levels, rings (marked with red arrows) were more prevalent in AS and SS cells. As O_2 concentrations are increased, parasites grown in AS RBCs appear identical to the parasites in AA RBCs. Parasites grown in SS RBCs also recover and appear similar to the wild type at hyperoxic conditions. Scale = 10 μm.

choice of HbF^+ cells is statistically higher than that at 21% O_2 ($P = .0047$, n = 10), indicating that at higher O_2 levels, parasites have a diminished preference for HbF^+ cells, which indicates a wider pool of host cells for the parasite to invade and proliferate within the SS cultures.

CB RBCs host superior proliferation of *B. divergens*

Cord blood (CB) RBCs are unique cells that differ from adult RBCs in membrane composition and biophysical properties, metabolism, and enzymatic profile[40] but most importantly, in their physiological concentration of HbF. Normal adult HbF is <1%, whereas most CB RBCs express >90% HbF, allowing us to investigate the impact of HbF on the proliferation of *B divergens*, away from the sickle RBC. However, depending on the time of delivery, CB can both vary in age and exhibit a wide range of HbF concentrations.

Viable merozoites were allowed to invade AA and CB cells and subsequently cultured at 5% and 21% O_2. Parasitemia was measured on days 1, 2, and 3. As shown in supplemental Figure 4A, starting from day 1, CB cells supported better growth of the parasite than AA cells. The differences became more prominent on day 2 when parasitemia in AA cells was 9.327% ± 1.983% and 12.860% ± 2.553% at 5% and 21% O_2, respectively, whereas in CB cells, it was 13.289% ± 1.333% and 17.658% ± 1.755% at 5%, and 21% O_2, respectively. The same trend was seen on day 3, beyond which the host cells had maximized hosting capacities and most cultures crashed on day 4. Thus, CB cells support higher growth than wild-type AA cells at both 5% and 21% O_2 ($P = .0066$, n = 9). IFC analysis of CB showed that the majority of cells were HbF^+ (red), whereas all cells were marked violet with anti-GPA (supplemental Figure 4B).

Using the (HbF-allophycocyanin (HbF-APC) antibody, we show that most CB samples had a high number of HbF^+ cells (65.611% ± 5.425%) (Supplementary Figure 4C)), which is significantly higher than adult AA cells (1.843% ± 0.41%). Under both O_2 conditions, we observed a positive correlation between CB HbF^+ cells and peak parasitemia (supplemental Figure 4E) (at 5% O_2, $R = 0.8421$, $P = .0044$; at 21% O_2, $R = 0.8246$, $P = .0059$).

Parasite subpopulation structure is affected by oxygenation

B divergens exists as 1N, 2N, 4N, and >4N parasite loads within the RBC, which changes based on the environment.[41] Mathematically, cells with higher N populations will yield more infective merozoites that can initiate new infection cycles, raising the levels of parasitemia as compared with cells with lower N and thus fewer merozoites. Therefore, when conditions are unfavorable, 1N host cells are predominant and when the parasite proliferates rapidly, 2N and 4N populations become more common. For a culture growing rapidly, its 1N:2N:4N and >4N is almost 33%:33%:33%.

We analyzed the subpopulation structure of parasites in the AA, AS, and SS cells under hypoxic (1%) and hyperoxic (21%) conditions. Figure 5A shows the percentage of the parasite population that are at 1N, 2N, and 4N genome equivalents on day 3 after invasion in different RBC genotypes grown at 1% O_2, whereas Figure 5B shows the same for parasites grown at 21% O_2. In both 1% and 21% O_2, parasites grown in AA cells maintain a similar proportion of 1N parasites (34.76% ± 1.623% and 35.581% ± 2.665% at 1% and 21% O_2, respectively). However, at 1% O_2, there is a significant increase in percentage of 1N parasites in AS cells (46.009% ± 3.84%, $P = .0076$) and SS cells (51.006% ± 4.229%; $P = .0016$) compared with AA cells, and these differences are statistically significant. The 2N subpopulations in AA, AS, and SS at 1% O_2 are 33.601% ± 0.778%, 33.68% ± 1.79%, and 27.465% ± 1.801%, respectively, whereas 4N and >4N are 31.52% ± 1.736%, 20.4% ± 2.12%, and 20.966% ± 2.988%, respectively. Therefore, at 1% O_2, 1N ring-stage parasites significantly increase in AS and SS cells with a concomitant reduction in 4N parasites in these cells, mirroring the low parasitemia obtained at 1% for these diseased genotypes. Figure 5C shows representative Giemsa-stained microscopic images of *B divergens* in AA, AS, and SS cells. As evident, at 1%, ring-stage 1N forms (marked with a red arrow) are predominant in AS and SS cells, whereas other subpopulation structures can be seen in AA cells.

When the O_2 environment is maintained at 21% (Figure 5B), the 1N population proportion of the parasites in AS and SS cells decreases to match that of the parasites in AA cells (35.581% ± 2.665% in AA vs 33.09% ± 2.586% in AS and 41.813% ± 3.258% in SS cells at 21% O_2). The 2N subpopulations in AA, AS, and SS cells at 21% O_2 are 36.182% ± 0.506%, 34.78% ± 0.89%, and 33.625% ± 1.89%, respectively, whereas 4N and >4N are 28.11% ± 2.54%, 32.27% ± 2.06%, and 23.977% ± 1.829%, respectively. Therefore, under favorable conditions (hyperoxia), parasites in AS cells exhibit the same subpopulation structure as parasites in AA cells, whereas those in SS cells have a near–wild-type AA subpopulation structure which reflects the near-normal parasite proliferation seen in SS cells at 21% O_2. This change in subpopulation structure in AS and SS cells is confirmed in Giemsa-stained microscopic images seen in Figure 5C. Under hypoxic conditions, red arrow marked ring-stage 1N predominates in AS and SS, whereas under hyperoxic conditions, 2N and 4N forms are abundantly present in all cultures.

Discussion

Host Hb genotype has been shown to play a protective role against malaria.[42-47] However, defense mechanisms against other intraerythrocytic parasites have not been fully explored. We had previously shown that under standard culture conditions, SS cells inhibited *Babesia* proliferation, whereas AS offered similar hosting as that of AA RBCs under standard culture conditions of 5% O_2/5% CO_2/90% N_2. However, *in vivo*, the O_2 concentration varies widely across the body from as low as 3% to > 15%.[31,48] Using hypoxic and hyperoxic conditions, we were able to discriminate differential effects of the 3 sickle Hb genotypes on parasite proliferation (Figure 1). Importantly, parasite hosting under hypoxic (1%) conditions varied greatly between AA cells vs AS and SS cells. When O_2 was restored to ≥ 5%, AS cells behaved similar to AA cells, leaving SS cells as the only genotype that offered a protection against *B divergens*. However, under hyperoxia (21%), even SS cells lost their protective ability against the parasite (Figure 1C), indicating the importance of studying parasite proliferation across various physiological environments. It is well known that HbS polymerization occurs at low O_2 when HbS shifts to the T-state, a conformation prone to polymerization, resulting in RBC sickling and allowing a plausible mechanism for the hypoxia-driven

inhibition of parasite growth seen in both AS and SS cells (Figure 1B-C). Electron microscopic evidence for Hb polymers has been demonstrated as the main reason for the inability of the malarial parasite to continue a productive life cycle in AS cells at low O_2 levels.[12] The differential ability of these genotypes to support the intraerythrocytic growth of *B divergens* lends support to this hypothesis. A major angle of our investigation was to identify the characteristics of SS host cells that allowed parasite invasion even under hypoxic conditions. SS cells are a heterogenous population with respect to the presence and amount of HbF, which in turn affect the shape and sickling propensity of the RBC.[49] The use of IFC can provide information regarding cellular morphology in addition to the detection of multiple fluorescent markers and is thus well suited to the study sickle RBCs and association of sickling with specific markers (supplemental Figure 3; Figure 4). We have developed an ML tool that can distinguish sickled cells from round cells in the population using various criteria (supplemental Table 1). Although some researchers have used IFC to determine "sickle" shape in SS cells, they have mostly relied on manual tools and most primarily on shape ratio. Our tool is unique in that it applies the ML module that allows for robust data collection while removing end-user bias and can be applied to multiple samples simultaneously. This allowed the unbiased classification of "nonsideways" cells within the SS population as "sickle" or "round" and further allowed us to link HbF positivity with the shape of the cell. Using this, we were able to show that *B divergens* almost exclusively develops in "round" cells and prefers HbF^+ cells over HbF^- cells (Figure 4). This can be explained by the reduction of mean cell HbS concentration in these HbF^+ SS cells, which is the main driver of Hb polymerization. To the best of our knowledge, this is the first study that uses IFC's ML extension to quantify the percentage of sickling in RBCs. Thus, hypoxia-driven sickling renders the host cell incapable of supporting robust parasite proliferation.[50]

In addition, the presence of HbF confers a superior parasite hosting capability, as CB RBCs supported a higher parasite proliferation compared with AA cells (supplemental Figure 4). Although CB RBCs are unique cells that differ in membrane composition and biophysical properties, Hb structure, metabolism, and enzymatic profile,[51,52] for our analysis, we focused on the main physiological difference in that HbF is present at a high concentration in CB cells (~80%) compared with AA cells (<1%).[53] Interestingly, prior reports for malaria indicated a potential resistance against the parasites by CB cells,[54,55] although a recent paper refuted these data and suggested that CB cells are equivalent to mature AA cells for malarial parasite multiplication.[56] Although we hypothesize that the presence of HbF is responsible for the improved parasite growth profile at both high and low O_2 levels, further work is required to elaborate whether other differences in CB RBCs also play a role in improving parasite outcomes in these cells.

Although HbF was an apparent conducive factor for parasite proliferation, there are other factors within the SS cells such as heightened oxidative stress that can inhibit the growth of *B divergens*. The instability of HbS causes repeated polymerization and depolymerization that lends itself to heightened production of ROS such as superoxide radicals, altering the redox environment of the SS RBC considerably from the wild-type AA RBC.[57-59] Such oxidative insults can lead to elevated amounts of ROS that has recently been postulated to interfere with malarial parasite functioning.[36] Thus, the elevated ROS levels in the host SS cells could also be responsible for the low parasitemia recorded (Figure 2). RBCs infected with *Plasmodium* have 2 sources of ROS, the degradation of Hb and the parasites mitochondrial electron transport chain.[60] In iAA cells, the only ROS signal appears coincident with parasite morphology (Figure 2C). However, for the SS genotype, many of the uninfected bystander cells show high ROS and upon infection, parasite-generated ROS contributed to the accumulated intra-RBC ROS (Figure 2D). To ensure their survival in these oxidative environments, we postulate that *B divergens*, similar to *Plasmodium*, must have several antioxidant machineries.[61]

Under optimal environmental conditions, *B divergens* uses a 33%:33%:33% ratio of 1N:2N:4N subpopulations to enable quick switches among the different morphological forms.[62] Analysis of the population structure under the different oxygenation conditions revealed a potential mechanism for the low parasitemia seen in hypoxic conditions (Figure 5). Parasites grown in AS and SS cells under 1% O_2 showed a higher proportion of 1N parasites, which was not seen in AA cells (Figure 5A). As the O_2 levels increased to 21%, *B divergens* in SS cells approached the typical equivalent ratios of the subpopulations. This is reflected in the overall increase in parasitemia seen in these cultures, as the number of merozoites released from 4N cells would be expected to increase parasitemia more significantly than lower genome equivalents. Although the hyperoxic culture conditions in SS cells did support higher proliferation overall, there was a clear lag in these cultures as compared with control AA cultures at the same O_2 levels (Figure 1D). Reasons for this delay are not clear and maybe linked to redox imbalance in SS cells but need further investigation.

To establish a comprehensive picture of the potential cellular mechanisms at play that permit differential parasite proliferation, we have constructed a model (visual abstract) that allows the discrimination of the various sickle genotypes, under different O_2 environments to serve as hosts for *B divergens*.

These studies further strengthen the role of the host-cell environment in dictating parasite success. Multiple mechanisms of resistance against the parasite are offered by SS and AS cells, especially in low-O_2 environments, but in turn, *B divergens* has evolved mechanisms to sense and invade more hospitable cells within the population and exploit subpopulation structures to enable survival. Understanding both the host and parasite mechanisms will allow the translation of research findings into future interventions to prevent and treat this blood-borne parasitic infection.

Acknowledgments

The authors acknowledge the help of Flow and Imaging Core at Lindsley F. Kimball Research Institute, New York Blood Center. They also thank Garry Cuneo, Field Application Scientist with Luminex for his help with IFC data analysis using ML and its classifiers.

Authorship

Contribution: D.B., M.S., K.Y., and C.A.L. conceived the experiments and wrote the manuscript; K.Y. and D.M. performed the clinical management of uninfected blood sample collection, including patient management and ethical clearance; D.B., M.S., M.R., and G.R. performed the parasite growth and proliferation

assays, and D.B., M.S., A.M., X.A., D.M., K.Y., and C.A.L. analyzed the results; and D.B. performed all redox assay and along with M.B.S, performed the IFC experiments and designed the ML tool.

Conflict-of-interest disclosure: The authors declare no competing financial interests.

ORCID profiles: D.B., 0000-0002-5966-419X; A.M., 0000-0002-1120-9593.

Correspondence: Cheryl A. Lobo, Department of Blood-Borne Parasites, Lindsley F. Kimball Research Institute, New York Blood Center, 310 East 67th St, New York, NY 10065; email: CLobo@Nybc.org.

References

1. Haldane JBS. The rate of mutation of human genes. *Hereditas*. 1949;35(S1):267-273.
2. Akide-Ndunge OB, Ayi K, Arese P. The Haldane malaria hypothesis: facts, artifacts, and a prophecy. *Redox Rep*. 2003;8(5):311-316.
3. Taylor SM, Parobek CM, Fairhurst RM. Haemoglobinopathies and the clinical epidemiology of malaria: a systematic review and meta-analysis. *Lancet Infect Dis*. 2012;12(6):457-468.
4. Gong L, Maiteki-Sebuguzi C, Rosenthal PJ, et al. Evidence for both innate and acquired mechanisms of protection from Plasmodium falciparum in children with sickle cell trait. *Blood*. 2012;119(16):3808-3814.
5. Beri D, Singh M, Rodriguez M, Yazdanbakhsh K, Lobo CA. Sickle cell anemia and Babesia infection. *Pathogens*. 2021;10(11):1435-1445.
6. Gray J, Zintl A, Hildebrandt A, Hunfeld KP, Weiss L. Zoonotic babesiosis: overview of the disease and novel aspects of pathogen identity. *Ticks Tick Borne Dis*. 2010;1(1):3-10.
7. Hildebrandt A, Gray JS, Hunfeld KP. Human babesiosis in Europe: what clinicians need to know. *Infection*. 2013;41(6):1057-1072.
8. Vannier EG, Diuk-Wasser MA, Ben Mamoun C, Krause PJ. Babesiosis. *Infect Dis Clin North Am*. 2015;29(2):357-370.
9. Dao AH, Eberhard ML. Pathology of acute fatal babesiosis in hamsters experimentally infected with the WA-1 strain of Babesia. *Lab Invest*. 1996;74(5):853-859.
10. Sevilla E, Gonzalez LM, Luque D, Gray J, Montero E. Kinetics of the invasion and egress processes of Babesia divergens, observed by time-lapse video microscopy. *Sci Rep*. 2018;8(1):14116.
11. Gong L, Parikh S, Rosenthal PJ, Greenhouse B. Biochemical and immunological mechanisms by which sickle cell trait protects against malaria. *Malar J*. 2013;12:317.
12. Archer NM, Petersen N, Clark MA, Buckee CO, Childs LM, Duraisingh MT. Resistance to Plasmodium falciparum in sickle cell trait erythrocytes is driven by oxygen-dependent growth inhibition. *Proc Natl Acad Sci U S A*. 2018;115(28):7350-7355.
13. Luzzatto L. Sickle cell anaemia and malaria. *Mediterr J Hematol Infect Dis*. 2012;4(1):e2012065.
14. Ord RL, Lobo CA. Human Babesiosis: pathogens, prevalence, diagnosis and treatment. *Curr Clin Microbiol Rep*. 2015;2(4):173-181.
15. Lobo CA, Singh M, Rodriguez M. Human babesiosis: recent advances and future challenges. *Curr Opin Hematol*. 2020;27(6):399-405.
16. Pal AC, Renard I, Singh P, et al. Babesia duncani as a model organism to study the development, virulence and drug susceptibility of intraerythrocytic parasites in vitro and in vivo. *J Infect Dis*. 2022;181.
17. Cursino-Santos JR, Singh M, Senaldi E, Manwani D, Yazdanbakhsh K, Lobo CA. Altered parasite life-cycle processes characterize Babesia divergens infection in human sickle cell anemia. *Haematologica*. 2019;104(11).
18. CDC. *Data and statistics on sickle cell disease*. Vol. 2022. Centers for Disease Control and Prevention; 2022.
19. Kato GJ, Piel FB, Reid CD, et al. Sickle cell disease. *Nat Rev Dis Primers*. 2018;4:18010.
20. Frenette PS, Atweh GF. Sickle cell disease: old discoveries, new concepts, and future promise. *J Clin Invest*. 2007;117(4):850-858.
21. Karkoska K, Louie J, Appiah-Kubi AO, et al. Transfusion-transmitted babesiosis leading to severe hemolysis in two patients with sickle cell anemia. *Pediatr Blood Cancer*. 2018;65(1):26734-26737.
22. Hatcher JC, Greenberg PD, Antique J, Jimenez-Lucho VE. Severe babesiosis in Long Island: review of 34 cases and their complications. *Clin Infect Dis*. 2001;32(8):1117-1125.
23. Krause PJ, Gewurz BE, Hill D, et al. Persistent and relapsing babesiosis in immunocompromised patients. *Clin Infect Dis*. 2008;46(3):370-376.
24. Burgess MJ, Rosenbaum ER, Pritt BS, et al. Possible transfusion-transmitted Babesia divergens-like/MO-1 infection in an Arkansas patient. *Clin Infect Dis*. 2017;64(11):1622-1625.
25. Mareedu N, Schotthoefer AM, Tompkins J, Hall MC, Fritsche TR, Frost HM. Risk factors for severe infection, hospitalization, and prolonged antimicrobial therapy in patients with babesiosis. *Am J Trop Med Hyg*. 2017;97(4):1218-1225.
26. Hutchings CL, Li A, Fernandez KM, et al. New insights into the altered adhesive and mechanical properties of red blood cells parasitized by Babesia bovis. *Mol Microbiol*. 2007;65(4):1092-1105.
27. Allred DR, Al-Khedery B. Antigenic variation and cytoadhesion in Babesia bovis and Plasmodium falciparum: different logics achieve the same goal. *Mol Biochem Parasitol*. 2004;134(1):27-35.

28. O'Connor RM, Allred DR. Selection of Babesia bovis-infected erythrocytes for adhesion to endothelial cells coselects for altered variant erythrocyte surface antigen isoforms. *J Immunol*. 2000;164(4):2037-2045.
29. Papageorgiou DP, Abidi SZ, Chang HY, et al. Simultaneous polymerization and adhesion under hypoxia in sickle cell disease. *Proc Natl Acad Sci U S A*. 2018;115(38):9473-9478.
30. Brezis M, Rosen S. Hypoxia of the renal medulla–its implications for disease. *N Engl J Med*. 1995;332(10):647-655.
31. Carreau A, El Hafny-Rahbi B, Matejuk A, Grillon C, Kieda C. Why is the partial oxygen pressure of human tissues a crucial parameter? Small molecules and hypoxia. *J Cell Mol Med*. 2011;15(6):1239-1253.
32. Di Liberto G, Kiger L, Marden MC, et al. Dense red blood cell and oxygen desaturation in sickle-cell disease. *Am J Hematol*. 2016;91(10):1008-1013.
33. Gorenflot A, Brasseur P, Precigout E, L'Hostis M, Marchand A, Schrevel J. Cytological and immunological responses to Babesia divergens in different hosts: ox, gerbil, man. *Parasitol Res*. 1991;77(1):3-12.
34. Lobo CA. Babesia divergens and Plasmodium falciparum use common receptors, glycophorins A and B, to invade the human red blood cell. *Infect Immun*. 2005;73(1):649-651.
35. Lobo CA, Rodriguez M, Cursino-Santos JR. Babesia and red cell invasion. *Curr Opin Hematol*. 2012;19(3):170-175.
36. Silva DGH, Belini Junior E, de Almeida EA, Bonini-Domingos CR. Oxidative stress in sickle cell disease: an overview of erythrocyte redox metabolism and current antioxidant therapeutic strategies. *Free Radic Biol Med*. 2013;65:1101-1109.
37. Sewchand LS, Johnson CS, Meiselman HJ. The effect of fetal hemoglobin on the sickling dynamics of SS erythrocytes. *Blood Cell*. 1983;9(1):147-166.
38. Christoph GW, Hofrichter J, Eaton WA. Understanding the shape of sickled red cells. *Biophys J*. 2005;88(2):1371-1376.
39. van Beers EJ, Samsel L, Mendelsohn L, et al. Imaging flow cytometry for automated detection of hypoxia-induced erythrocyte shape change in sickle cell disease. *Am J Hematol*. 2014;89(6):598-603.
40. Zhurova M, Akabutu J, Acker J. Quality of red blood cells isolated from umbilical cord blood stored at room temperature. *J Blood Transfus*. 2012;2012:102809.
41. Cursino-Santos JR, Alhassan A, Singh M, Lobo CA. Babesia: impact of cold storage on the survival and the viability of parasites in blood bags. *Transfusion*. 2014;54(3):585-591.
42. Petersen JEV, Saelens JW, Freedman E, et al. Sickle-trait hemoglobin reduces adhesion to both CD36 and EPCR by Plasmodium falciparum-infected erythrocytes. *PLoS Pathog*. 2021;17(6):e1009659.
43. Saelens JW, Petersen JEV, Freedman E, et al. Impact of sickle cell trait hemoglobin on the intraerythrocytic transcriptional program of Plasmodium falciparum. *mSphere*. 2021;6(5):e0075521.
44. Diakite SA, Ndour PA, Brousse V, et al. Stage-dependent fate of Plasmodium falciparum-infected red blood cells in the spleen and sickle-cell trait-related protection against malaria. *Malar J*. 2016;15(1):482.
45. Lopera-Mesa TM, Doumbia S, Konate D, et al. Effect of red blood cell variants on childhood malaria in Mali: a prospective cohort study. *Lancet Haematol*. 2015;2(4):e140-149.
46. Glushakova S, Balaban A, McQueen PG, et al. Hemoglobinopathic erythrocytes affect the intraerythrocytic multiplication of Plasmodium falciparum in vitro. *J Infect Dis*. 2014;210(7):1100-1109.
47. Taylor SM, Cerami C, Fairhurst RM. Hemoglobinopathies: slicing the Gordian knot of Plasmodium falciparum malaria pathogenesis. *PLoS Pathog*. 2013;9(5):e1003327.
48. Mata-Greenwood E, Goyal D, Goyal R. Comparative and experimental studies on the genes altered by chronic hypoxia in human brain microendothelial cells. *Front Physiol*. 2017;8:365.
49. Steinberg MH, Chui DH, Dover GJ, Sebastiani P, Alsultan A. Fetal hemoglobin in sickle cell anemia: a glass half full? *Blood*. 2014;123(4):481-485.
50. Yi W, Bao W, Rodriguez M, et al. Robust adaptive immune response against Babesia microti infection marked by low parasitemia in a murine model of sickle cell disease. *Blood Adv*. 2018;2(23):3462-3478.
51. Oski FA. The unique fetal red cell and its function. E. Mead Johnson Award address. *Pediatrics*. 1973;51(3):494-500.
52. Brugnara C, Platt O. *Nathan and Oski's hematology of infancy and childhood*. Saunders; 2003.
53. Stiene-Martin EA, Lotspeich-Steininger CA, Koepke JA. *Clinical hematology: principles, procedures, correlations*. Lippincott Williams & Wilkins; 1998.
54. Pasvol G, Weatherall DJ, Wilson RJ, Smith DH, Gilles HM. Fetal haemoglobin and malaria. *Lancet*. 1976;1(7972):1269-1272.
55. Pasvol G, Weatherall DJ, Wilson RJ. Effects of foetal haemoglobin on susceptibility of red cells to Plasmodium falciparum. *Nature*. 1977;270(5633):171-173.
56. Archer NM, Petersen N, Duraisingh MT. Fetal hemoglobin does not inhibit Plasmodium falciparum growth. *Blood Adv*. 2019;3(14):2149-2152.
57. Antwi-Boasiako C, Dankwah GB, Aryee R, Hayfron-Benjamin C, Donkor ES, Campbell AD. Oxidative profile of patients with sickle cell disease. *Med Sci*. 2019;7(2):17-25.
58. Hebbel RP, Morgan WT, Eaton JW, Hedlund BE. Accelerated autoxidation and heme loss due to instability of sickle hemoglobin. *Proc Natl Acad Sci U S A*. 1988;85(1):237-241.
59. Nolfi-Donegan D, Pradhan-Sundd T, Pritchard KA Jr, Hillery CA. Redox signaling in sickle cell disease. *Curr Opin Physiol*. 2019;9:26-33.

60. Egwu CO, Augereau JM, Reybier K, Benoit-Vical F. Reactive oxygen species as the brainbox in malaria treatment. *Antioxidants (Basel)*. 2021;10(12):1872-1896.

61. Muller S. Role and regulation of glutathione metabolism in plasmodium falciparum. *Molecules*. 2015;20(6):10511-10534.

62. Cursino-Santos JR, Singh M, Pham P, Rodriguez M, Lobo CA. Babesia divergens builds a complex population structure composed of specific ratios of infected cells to ensure a prompt response to changing environmental conditions. *Cell Microbiol*. 2015;18(6).